WOOD RESEARCH
53 (2): 2008
57-66

DETECTION OF KNOTS USING X-RAY TOMOGRAPHIES AND DEFORMABLE CONTOURS WITH SIMULATED ANNEALING

Aguilera C. Cristhian, Ricardo Sanchez
Dpt. Ing. Eléctrica, Universidad de Concepción, Concepción, Chile

Erik Baradit
Depto. de Física, Universidad del Bio-Bio, Concepción, Chile

ABSTRACT

The recognition of defects in the wood manufacture process is ever more necessary and fundamental. However, the utilization of robust techniques that will allow these machines to provide a high degree of reliability is still a matter for study. Images obtained with X-rays and other techniques are already being used in the wood industry. However, the challenge remains to develop robust detection methods for different species and considering their distinct conditions. In this article, we present a defect segmentation method, initially developed to detect wood knots in *Pinus radiata*, based on images taken with X-ray computerized tomographies. This process uses deformable contour techniques (snakes), basing their evolution on a simulated annealing search method. The results obtained are highly satisfactory with respect to other approaches and the methodology appears to be a robust method of defect detection in round lumber under different conditions.

KEY WORDS: image processing, X-rays, *Pinus radiata*

INTRODUCTION

The knowledge of the internal structure of a material is important information and is highly relevant when it is necessary to optimize a final product or improve its quality indexes (Benson et al. 1982). In the case of the wood industry, for example, the exact knowledge of the internal structure of a log or round lumber such as density and the location of its internal defects is an important economic advantage (Harless et al. 1991). Internal characteristics of materials have been studied with different non-destructive techniques, including ultrasound (Sandoz 1993), microwaves (Martin 1987, King 1991, Gapp and Mallick 1995, Baradit 2006, Lundgren et al. 2007), gamma rays, X-rays, nuclear magnetic resonance (NMR) and, lately, artificial vision techniques (Thomas and Mili 2006). X-rays

have been used to examine the internal characteristics of many materials (Funt and Bryant 1987, Zhu et al. 1996, Rojas et al. 2005, Eriksson et al. 2006).

An X-ray computerized tomography reflects variations in the density of an object or body. Only gamma ray and X-ray sensors reveal the shape of a log below the bark, allowing the detection of macroscopic and microscopic aspects of the wood. At the same time, an important number of visualization and segmentation techniques have been developed that have been largely successful, enabling their incorporation in state-of-the-art medical equipment.

In the wood industry, some applications have been found that allow the recognition of different types of defects in the raw material (Sarigul et al. 2001, Oja et al. 1998). Methods for measuring moisture (Sandoz 1993), density (Lindgren 1991), and labeling (Schmoldt et al. 2000) have also been developed. Some works have been presented related to knots (Taylor et al. 1984, Wagner et al. 1989). However, the automated recognition of defects in shape in the manufacture process is ever more necessary and fundamental. The emphasis on the use of automated recognition techniques relying on digital images is growing constantly and such capabilities are currently being incorporated into an important amount of equipment. However, the utilization of robust detection techniques that allow a high degree of reliability from these machines is still a matter for study. The use of X-ray images for wood applications has been disseminated in several works (Grundberg and Gronlund 1997). For example, Sepúlveda and Kline (2003) recently proposed a method for predicting the orientation of fibers using X-rays, whereas Rojas et al. (2005) explored the internal physical properties of sugar maple logs. Other efforts have focused on the development of industrial prototypes for applications in sawed lumber (Zhu et al. 1996). Nonetheless, the challenge remains to develop robust automatic detection methods for different wood species and their conditions.

In the specific case of wood, methods have been developed for both internal as well as external inspection (Thomas and Mili 2006). Diverse internal inspection techniques have been applied, including the segmentation of images from X-ray tomographies. One of the methods used is aimed at contour deformations (snakes). However, most of the techniques used to follow these contours are based or guided, principally relying on the intensity of the image and the distribution characteristics of the points and elasticity of the contour defined in terms of energies. The search for solutions has been confronted from local and global optimization points of view. This has given good results when the images or objects do not have strong irregularities or undesirable points of attraction or repulsion. When this is not the case, the segmentation produced tends to smooth the borders of the objects or to deviate the contour to regions that do not correspond to the defect to be isolated, and precise definitions of the contours are not obtained, particularly in images coming from tomographies of wood with, for example, a high moisture content.

In this work, we develop an automatic segmentation method for images from X-ray computerized tomographies using deformable contours that base their guided movement on the image intensity and that also incorporate a random component based on simulated annealing for the evolution of its points. The first results of the analysis of these 2D images for the segmentation of singularities in logs are presented herein. In order to validate the proposed technique and the results shown, we inspected *Pinus radiata* logs to isolate or segment, in a first instance, knots.

MATERIAL AND METHODS

A deformable contour or snake (Kass et al. 1988) is a parametric curve of the type

$$u(s) = (x(s), y(s)) \tag{1}$$

Where x(s) and y(s) are coordinates along the contour and $s \in [0,1]$. These contours are influenced by internal and external forces and forces typically related to the /gradient of the intensity of the image, mathematically:

$$E_{snake} = \int_0^1 [E_{\text{int}}(u(s)) + E_{ext}(u(s)) + E_{img}(u(s))]\, ds \tag{2}$$

where:

$$E_{int}(x) = a(s)|x_s(s)|^2 + \beta(s)|x_{ss}(s)|^2$$

Tension *Stiffness*

$E_{ext}(x) =$ *Shape Energy , Measure of external constraints either from higher level shape information or user applied energy*

$$E_{img} = -\alpha\|\nabla I\|^2$$

The internal energy, E_{int}, with alpha and beta parameters, controls the tension and rigidity of the contour; E_{ext} represents measures or external considerations with respect to the shape of the contour; and E_{img} is the force related to the gradient of the image given a Gaussian-type convolution filter. The contour is initially located near the object to be segmented in the image and forces of attraction and repulsion generated by internal, external, and image forces deform the contour until it is surrounded, thereby isolating the object with respect to the overall image (Fig. 1).

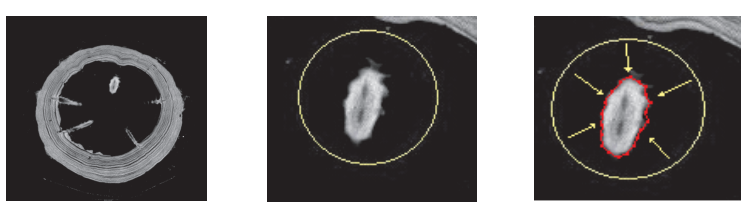

(a) (b) (c)

Fig. 1: Evolution of a deformable contour: (a) initial image, (b) initial contour, (c) final contour

Different images taken with X-ray tomography were used. These are 2D images of selected *Pinus radiata* logs cut into 1-meter-long sections between 30 and 35cm in diameter. The logs selected were remnants from a pruning treatment. The images were obtained using the cut-to-cut technique with a 10mm sweep and 5mm ray width; a total of 90 images were analyzed.

As shown in Fig. 1, the contour near the object to be segmented is attracted and

deformed by the force of the image until the contour completely surrounds the object. The forces coming from the gradient of the images guide the contour until it is located around the object's borders. In Fig. 1, we can see the evolution of the contour for the segmentation of knots in *Pinus radiata* wood. We can see that this method can be very strongly influenced by other objects in the image, or by points of intensities not related to the object, producing a poor segmentation of the defect. In particular, Fig. 1 shows the existence of forces of attraction in other regions of the contour not associated with the knot (in this case, growth rings) and in zones or points that influence the contour, thereby causing a poor final segmentation. Several methods, both global and local, have been applied to minimize the functional energy (2).

Fig. 2 presents a tomographic image of a log: 2a shows the tomographic image itself, in which two knots and the appearance of a third knot can clearly be seen at the bottom of the image; 2b shows the enlarged sector of the image corresponding to a particular knot. Fig. 2c represents the gradient of the image, the most intense points represent the greatest values of the gradient. These forces guide the contour around the knot in order to completely isolate it, as shown in Fig. 2d. One of the problems to confront is to identify, given the energy function and initial contour, the location of each new point of the contour. This can be done with different search algorithms.

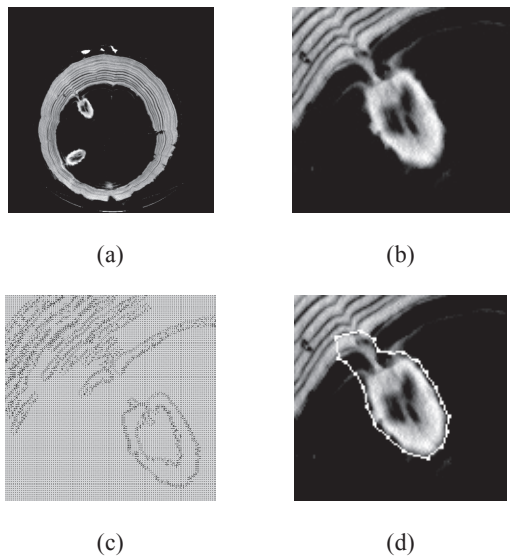

Fig. 2: (a) Tomographic image, (b) knot (enlargement), (c) gradient of the image, (d) segmentation through a deformable contour

Simulated annealing is a stochastic optimization technique introduced by Kirkpatrick et al. (1983). This algorithm begins by selecting an initial solution and later generating a new state, randomly generating a new solution in the neighborhood of the current solution; this is called a neighbor solution. This new state is evaluated and compared with the

previous solution. If the new state is better than the previous one, it is accepted; but if it is not, it is accepted or rejected with some probability. The probability of accepting a new state is given by:

$$e^{-\Delta E / T} > R \tag{3}$$

With: ΔE: Difference between the present and the candidate solutions
T: Temperature
R: Random uniform number between [0,1]

ΔE reflects the change in the objective function and T is the current temperature. This last expression is commonly known as the Cooling Schedule and several types of cooling can be found in the literature (exponential, sigmoid, linear, etc.), as can different conditions of terms for the algorithm.

Two methods of minimization have been used in this work: one based on the *greedy algorithm* and the other on *simulated annealing*. In both methods, the center of the mass of the knot is used to locate the initial contour. Masks of 5x5 pixels are used in both cases for each of the contour's points.

RESULTS AND DISCUSSION

According to the above description and using the energy functions described in (1), we proceeded to analyze the images from the X-ray computerized tomographies of logs with different characteristics. To carry out these experiments, we used discreet versions of the energy functions and a local optimization algorithm based on the greedy algorithm and another based on simulated annealing.

The assays were carried out with tomographies of various logs using a medical scanner. In total, 90 images were analyzed. The most relevant results are shown in the following figures.

Fig. 3 shows a sequence of images revealing the evolution of the knots inside a log. On the left, we can see the images of the complete log and, on the right, an enlargement of the image corresponding to a single knot. Fig. 4 shows the situation of a knot that appears to be an isolated object in the image: 4a shows the result of the segmentation using the greedy algorithm and 4b using simulated annealing. In both cases, the segmentation gives good results; the contour becomes deformed around the knot, isolating it completely. It should be noted here that, in this case, the knot in the image appears to be totally isolated and there are no objects that distort the contour deformation. Fig. 5 presents the result of the segmentation in a case in which the knots are confused with the growth rings: 6a shows the result when using the greedy algorithm and 5b the result with simulated annealing. In this case, a considerable difference can be appreciated between the two methods. The energy gradients generated by the image of the growth rings tend to position the contour away from the knot. However, with simulated annealing, due to its characteristic random exploration, it tends to better segment the knot in general. In Fig. 6, the situation is more critical. In these images the knots are confused with the growth rings; in fact, the knot is only partially visible in the tomographic image, and it appears to be an object with different geometric characteristics than those visible in the previous images. Fig. 6a shows the result of the evolution of the contour with the greedy algorithm; here the algorithm clearly does

not surround the knot correctly and the results of the segmentation are extremely poor. Nonetheless, in Fig. 6b, with simulated annealing and thanks to a wider exploration, the general results are perceptibly better.

As we can see in the figures presented herein, in some situations the images obtained by X-ray computerized tomographies facilitate segmentation. Nevertheless, in other situations, the segmentation is seriously complicated by confusion with other objects in the image. In particular, growth rings and other objects distract the contours. In such cases, a classical optimization algorithm such as the greedy algorithm does not provide good results, principally due to the tendency for local minima. However, simulated annealing provides a more robust method for presenting better results in these situations.

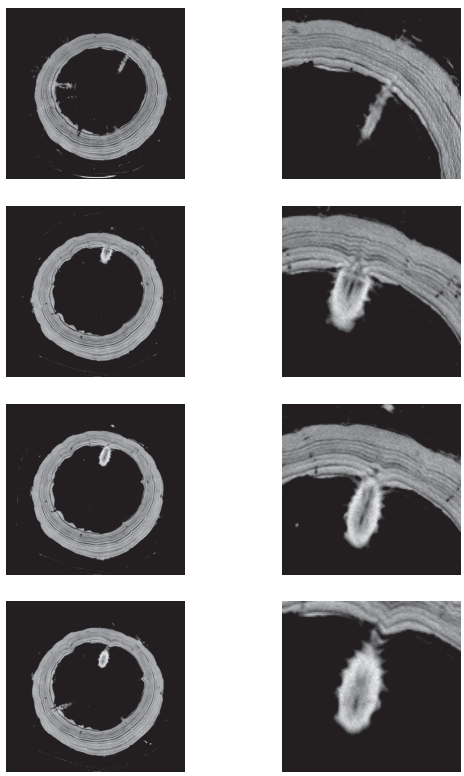

Fig. 3: Tomography of a log: on the left, the transversal cut; on the right, the enlarged image

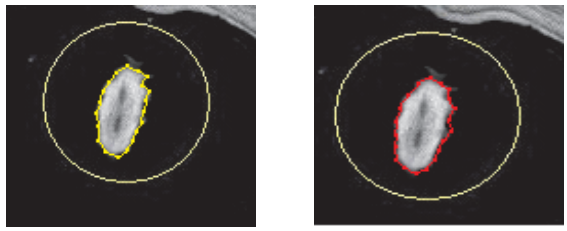

(a) (b)

Fig. 4: Evolution of an initial contour around an isolated knot: (a) greedy algorithm, (b) simulated annealing algorithm

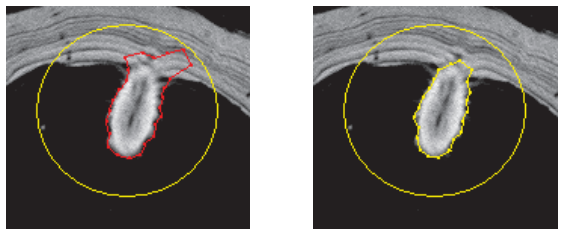

(a) (b)

Fig. 5: Evolution of an initial contour around a knot with interference from growth rings: (a) greedy algorithm, (b) simulated annealing algorithm

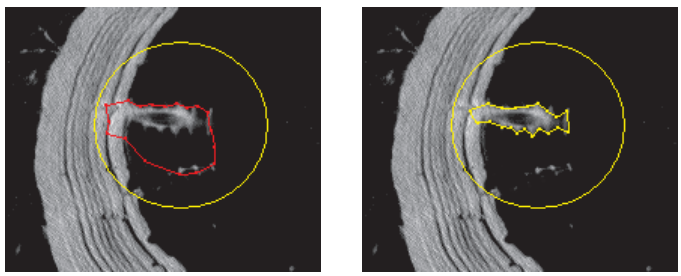

(a) (b)

Fig. 6: Evolution of an initial contour around a knot with interference from growth rings: (a) greedy algorithm, (b) simulated annealing algorithm

CONCLUSIONS

Given our results, we can conclude that the method presented is a very good alternative for knot segmentation. The use of simulated annealing allows much more precise segmentation of knots with greater irregularities in the images. Nonetheless, the initial position of the deformable contour is of vital importance for a good identification. We can also use the results obtained to infer that both excessive humidity content in the logs and growth rings present inconveniences. The latter presents a great challenge since the knot shows up in the images obtained with X-rays both in isolation and confused with other objects. In the second case, additional information, for example morphological information on the knots, can be incorporation into the countour's energy function that describes the force of the image, offering a very good alternative. The cases examined correspond to segmentation by X-ray computerized tomography for logs having distortions due mainly to their storage; this causes the density of the material to increase, which then has an affect on the images. This case is of great interest for the wood industry. However, this technique can also be used in other situations such as the study of other defects in logs. The authors are currently developing 3D techniques and a way to reduce the method's computerization costs that were were not considered in this first study.

REFERENCES

1. Baradit, E., Aedo, R., Correa, J., 2006: Knot detection in Wood using microwaves, Wood Science and Technology: 40(2): 118-123
2. Benson-Cooper, D., Knowles, R., Thompsom, F., Cown., 1982: Detection of defaults in logs, Forest Reserach Institute of New Zeeland 8(1): 9-12
3. Eriksson, J., Johansson, H., Danvind, J., 2006: Numerical Determination of Diffusion Coefficients in Wood Using Data From CT-Scanning, Wood and Fiber Science, 38(2): 334-344
4. Funt, B., Bryant, E., 1987: Detection of internal log defects by automatic interpretation of computer tomography images, Forest Product Journal 37(1): 56-62
5. Gapp, V., Mallick, G., 1995: Capteur intelligent pour la mesure de la humdité dans le matériau par technique micro-ondes, Journées Nationales micro-ondes, Paris 73(3): 53-57
6. Grundberg, S., Gronlund, A., 1997: Simulated grading of log with an x-ray log scanner-grading accuracy compared with manual grading, Lulea University of Technology-Scandinavian Journal Forest, 12(1): 70-76
7. Harless, T., Wagner, F., Steele, P., Taylor, F., Yadama, V., McMillin, C., 1991: Methodology for locating defect within hardwood logs and determining their impact on lumber value yield, Forest Product Journal, 41(4): 25-30
8. Kass, M., Wikins, K., Terzopoulos, D., 1988: Snake: Active Contour Model, International Journal of Computer Vision, 4(1): 321-331
9. King, R., 1991: Measurement of basic weight and moisture content of composite board using microwave, VIII th Int. Symp. On non-destructive testing of wood Pp. 21-32
10. Kirkpatrick, S., Gelatt, C., Vecchi, M., 1983: Optimization by Simulated Annealing, Science 220(4598): 671–680
11. Lindgren, L., 1991: Medical CAT-Scanning: x-ray CT-numbers and their relation to wood density, Wood Science and Technology (25): 341-349

12. Lundgren, N., Brännström, M., Hagman, O., Oja, J., 2007: Predicting the Strength of Norway Spruce by Microwave Scanning: A Comparison with Other Scanning Techniques, Wood and Fiber Science 39(1): 167-172
13. Martin, P., 1987: Evaluation of wood characteristics. Internal scanning off the material by microwaves, Wood Sciences and Technology 21(4): 361-371
14. Oja, J., Grundberg, S., Gronlund, A., 1998: Measuring the outer shape of pinus sylvestris saw logs with an x-ray log scanner, Scandinavian journal forest, 13: 340-347
15. Rojas, G., Hernández, R., Condal, A., Verret, D., Beauregard, R., 2005: Exploration of the Physical Properties of Internal Characteristics of Sugar Maple Logs and Relationships with CT Images, Wood and Fiber Science 37(4): 591-604
16. Sarigul, E., Abbott, L., Schmoldt, D., 2001: Nondestructive rule-based defect detection and indentification system in CT images of hardwood logs, Review of Progress in Nondestructive Evaluation 20: 1936-1943
17. Sandoz, J., 1993: Moisture content and temperature effect on ultrasound timber grading, Wood Science and Technology 27(5): 373-380
18. Schmoldt, D., He, J., Abbort, A., 2000: Automated Labeling of log feature in CT imagery of multiple hardwood species, Wood and Fiber Science 32: 287-300
19. Sepulveda, P., Kline, D., 2003: Prediction of Fiber Orientation in Norway Spruce Logs Using an X-Ray Log Scanner: A Preliminary Study, Wood and Fiber Science, Issue Volume 35, Number 35(3): 421-428
20. Taylor, F., Wagner, F., McMillin, C., Morgan, I., Hopkins, F., 1984: Locating Knots by Industrial Tomography, Forest Product Journal 34(5): 42-46
21. Thomas, L., Mili, L., 2006: Defect Detection on Hardwood Logs Using Laser Scanning, Wood and Fiber Science 38(4): 243-246
22. Wagner, F., Roder, F., 1989: Ultrafast CT scanning of an oak log for internal defect, Technical Note, Forest Product Journal 39(11/12): 62-64
23. Zhu, D., Conners, R., Schmoldt, D., Araman, P., 1996: A prototype Vision System for Analyzing CT Imagery of Hardwood Logs. IEEE Transactions on Systems, Man and Cybernetics—Part B: Cybernetics 26(4): 522-532

Aguilera C. Cristhian
Depto. Ing. Eléctrica
Universidad de Concepción
Victor Lamas 1290
Casilla 160-C
Concepción
Chile
E-mail: cristhia@ubiobio.cl

Ricardo Sanchez
Depto. Ing. Eléctrica
Universidad de Concepción
Victor Lamas 1290
Casilla 160-C
Concepción
Chile

Erik Baradit
Depto. de Física
Universidad del Bio-Bio
Av. Collao 1202
Casilla 5-C
Concepción
Chile